J|A|C|S
ARTICLES
Published on Web 11/11/2006

Characterization of Manganese(V)−Oxo Polyoxometalate Intermediates and Their Properties in Oxygen-Transfer Reactions

Alex M. Khenkin,[†] Devesh Kumar,[‡] Sason Shaik,*[,‡] and Ronny Neumann*[,†]

Contribution from the Department of Organic Chemistry, Weizmann Institute of Science, Rehovot, Israel 76100, and Department of Organic Chemistry and the Lise Meitner-Minerva Center for Computational Quantum Chemistry, The Hebrew University, Jerusalem, Israel 91904

Received June 1, 2006; E-mail: sason@yfaat.ch.huji.ac.il; Ronny.Neumann@weizmann.ac.il

Abstract: A manganese(III)-substituted polyoxometalate, $[\alpha_2\text{-}P_2Mn^{III}(L)W_{17}O_{61}]^{7-}$ ($P_2W_{17}Mn^{III}$), was studied as an oxidation catalyst using iodopentafluorobenzene bis(tifluoroacetate) ($F_5PhI(TFAc)_2$) as a monooxygen donor. Pink $P_2W_{17}Mn^{III}$ turns green upon addition of $F_5PhI(TFAc)_2$. The ^{19}F NMR spectrum of $F_5PhI(TFAc)_2$ with excess $P_2W_{17}Mn^{III}$ at −50 °C showed the formation of an intermediate attributed to $P_2W_{17}Mn^{III}-F_5PhI(TFAc)_2$ that disappeared upon warming. The ^{31}P NMR spectra of $P_2W_{17}Mn^{III}$ with excess $F_5PhI(TFAc)_2$ at −50 and −20 °C showed a pair of narrow peaks attributed to a diamagnetic, singlet manganese(V)−oxo species, $P_2W_{17}Mn^{V}{=}O$. An additional broad peak at −10.6 ppm was attributed to both the $P_2W_{17}Mn^{III}-F_5PhI(TFAc)_2$ complex and a paramagnetic, triplet manganese(V)−oxo species. The electronic structure and reactivity of $P_2W_{17}Mn^{V}{=}O$ were modeled by DFT calculations using the analogous Keggin compound, $[PMn^{V}{=}OW_{11}O_{39}]^{4-}$. Calculations with a pure functional, UBLYP, showed singlet and triplet ground states of similar energy. Further calculations using both the UBLYP and UB3LYP functionals for epoxidation and hydroxylation of propene showed lowest lying triplet transition states for both transformations, while singlet and quintet transition states were of higher energy. The calculations especially after corrections for the solvent effect indicate that $[PMn^{V}{=}OW_{11}O_{39}]^{4-}$ should be highly reactive, even more reactive than analogous $Mn^{V}{=}O$ porphyrin species. Kinetic measurements of the reaction of $P_2W_{17}Mn^{V}{=}O$ with 1-octene indicated, however, that $P_2W_{17}Mn^{V}{=}O$ was less reactive than a $Mn^{V}{=}O$ porphyrin. The experimental enthalpy of activation confirmed that the energy barrier for epoxidation is low, but the highly negative entropy of activation leads to a high free energy of activation. This result originates in our view from the strong solvation of the highly charged polyoxometalate by the polar solvent used and adventitious water. The higher negative charge of the polyoxometalate in the transition versus ground state leads to electrostriction of the solvent molecules and to a loss of degrees of freedom, resulting in a highly negative entropy of activation and slower reactions.

Introduction

A subclass of polyoxometalate compounds is one where a transition metal, often in a lower oxidation state, substitutes for a tungsten− or molybdenum−oxo group at the polyoxometalate surface (Figure 1). The substituting metal center is thus pentacoordinated by the "parent" polyoxometalate. The octahedral coordination sphere is completed by an additional sixth labile ligand, L (usually L = H_2O). The lability of the sixth ligand allows the interaction of the substituting transition-metal atom with an oxidant, leading to active oxidizing species. In analogy to metallorganic chemistry the "pentadentate" polyoxometalate can act as an inorganic ligand. As such, transition-metal-substituted polyoxometalates were early on referred to as "inorganic metalloporphyrins", and comparisons of the catalytic activity of the two systems were made, using iodosobenzene and pentafluoroiodosobenzene as oxidants.[1] Especially, the manganese(II/III)-substituted Keggin, $[PMn^{II}(H_2O)W_{11}O_{39}]^{5-}$, and Wells−Dawson, $[\alpha_2\text{-}P_2Mn^{III}(Br)W_{17}O_{61}]^{7-}$, polyoxometalates, Figure 1, showed good activity and high selectivity for the epoxidation of alkenes and some activity for the hydroxylation of alkanes that compared well to the activity of the manganese(III) tetrakis(2,6-dichlorophenyl)porphyrin, especially upon factoring in the higher stability of the polyoxometalates.

Manganese-substituted polyoxometalates have also been used as catalysts with other oxidants such as ozone, hydrogen peroxide, and nitrous oxide, although the preliminary research appeared to indicate that the active oxidizing intermediate was not likely a manganese−oxo species.[2] If one takes the poly-

[†] Weizmann Institute of Science.
[‡] The Hebrew University.

(1) (a) Hill, C. L.; Brown, R. B. *J. Am. Chem. Soc.* **1986**, *108*, 536−537. (b) Mansuy, D.; Bartoli, J. F.; Battioni, P.; Lyon, D. K.; Finke, R. G. *J. Am. Chem. Soc.* **1991**, *113*, 7222−7229.
(2) (a) Neumann, R.; Khenkin, A. M. *Chem. Commun.* **1998**, 1967−1968. (b) Neumann, R.; Gara, M. *J. Am. Chem. Soc.* **1994**, *116*, 5509−5510. (c) Neumann, R.; Gara, M. *J. Am. Chem. Soc.* **1995**, *117*, 5066−5074. (d) Neumann, R.; Juwiler, D. *Tetrahedron* **1996**, *47*, 8781−8788. (e) Boesing, M.; Noeh, A.; Loose, I.; Krebs, B. *J. Am. Chem. Soc.* **1998**, *120*, 7252−7259. (f) Ben-Daniel, R.; Weiner, L.; Neumann, R. *J. Am. Chem. Soc.* **2002**, *124*, 8788−8789.

10.1021/ja0638455 CCC: $33.50

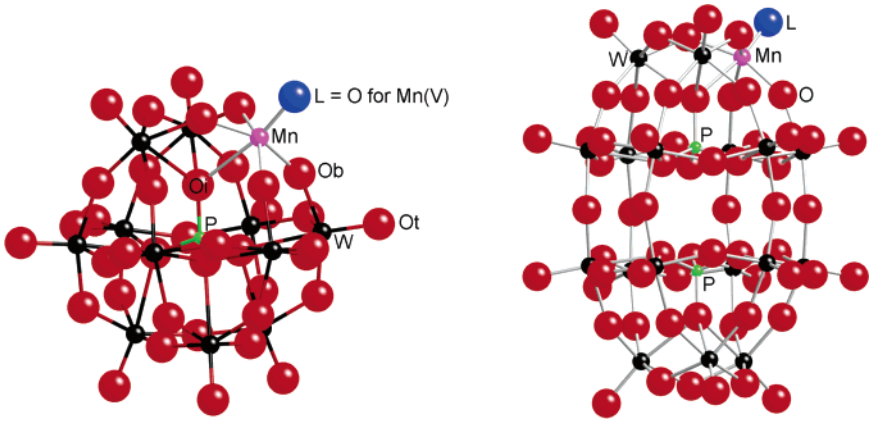

Figure 1. Ball and stick models of Keggin, $[PMn(L)W_{11}O_{39}]^{5-}$ (left), and Wells−Dawson, $[\alpha_2\text{-}P_2Mn(L)W_{17}O_{61}]^{7-}$ (right), polyoxometalates.

oxometalate− "inorganic metalloporphyrin" analogy a step further, one should of course discuss also the active intermediate species for oxygen transfer. In this context, for iron-based compounds the reactivity of the iron(IV)−oxo porphyrin cation radical species has been well elucidated.[3] It has been computationally shown that a formally analogous iron(V)−oxo polyoxometalate will also be highly reactive although this intermediate has apparently not yet been accessed.[4] The active intermediate species in the manganese porphyrin system has been rather extensively studied over the years, and it has been found that both manganese(IV)−oxo and manganese(V)−oxo species are competent oxygen-transfer intermediates although the latter is more reactive.[5] Various other high manganese(V)−oxo species based on salen,[6] corrole,[7] corrolazine,[8] and other nitrogen-based ligands have been identified.[9] Not surprisingly, the more active manganese(V)−oxo species with porphyrin, salen, and triazocyclononane ligands have only been observed as transient intermediates, whereas the less or nonactive manganese(V)−oxo species with corrole, corrolazine, and cyclic tetraamido ligands have been isolated.

Although some manganese(IV)−oxo-containing polyoxometalates have been identified,[10] they are inefficient oxygen donors and thus highly unlikely to be the reactive intermediates in manganese-substituted-polyoxometalate-catalyzed reactions. To date, manganese(V)−oxo polyoxometalate species, reasonable candidates for such a reactive intermediate,[4] have been neither isolated nor identified as transient reactive intermediates in manganese-substituted-polyoxometalate-catalyzed oxidations. In this paper we provide our combined experimental and computational results concerning such manganese(V)−oxo intermediates and their C−H hydroxylation and C═C epoxidation reactivity patterns.

Results and Discussion

The experimental study was carried out using $[\alpha_2\text{-}P_2Mn^{III}(H_2O)W_{17}O_{61}]^{7-}$ ($P_2W_{17}Mn^{III}$) with the Wells−Dawson structure as the polyoxoanion catalyst and iodopentafluorobenzene bis(tifluoroacetate) ($F_5PhI(TFAc)_2$) as the oxygen donor. The rationale behind these choices was that $P_2W_{17}Mn^{III}$ had two phosphorus atoms with different chemical environments that could be effectively utilized in ^{31}P NMR studies and that the $F_5PhI(TFAc)_2$ is freely soluble contrary to its iodosobenzene counterparts (PhIO and F_5PhIO), simplifying mechanistic studies and also allowing the use of ^{19}F NMR as a spectroscopic probe. Since $F_5PhI(TFAc)_2$ had not been specifically used as an oxygen donor in catalyzed reactions, the first step in the research was the purview of $P_2MnW_{11}/F_5PhI(TFAc)_2$ reactions. In Table 1 we present the yields of representative reactions at essentially complete conversion of $F_5PhI(TFAc)_2$.

The results showed that catalyses by $P_2W_{17}Mn^{III}/F_5PhI(TFAc)_2$ were largely similar to those described for $P_2W_{17}Mn^{III}$/PhIO in the literature[1b] with some differences. The following conclusions may be drawn: (i) The oxidation of sulfides was fairly facile; by the use of thianthrene oxide as a probe substrate, it appears that the active oxidizing species should not be described as electrophilic or nucleophilic since the disulfoxide and sulfone were formed in equivalent amounts.[11] (ii) The

(3) (a) Ortiz de Montellano, P. R., Ed.; *Cytochrome P450: structure, mechanism and biochemistry*, 2nd ed.; Plenum Press: New York, 1995. (b) Ortiz de Montellano, P. R., Ed.; *Cytochrome P450: structure, mechanism and biochemistry*, 3rd ed.; Kluwer Academic/Plenum Publishers: New York, 2005. (c) Groves, J. T. *Proc. Natl. Acad. Sci. U.S.A.* **2003**, *100*, 3569−3574. (d) Sono, M.; Roach, M. P.; Coulter, E. D.; Dawson, J. H. *Chem. Rev.* **1996**, *96*, 2841−2887. (e) Groves, J. T.; Han, Y. Z. Models and mechanisms of Cytochrome P450 action. In ref 3a, Chapter 1, p 3. (f) Harris, D. L. *Curr. Opin. Chem. Biol.* **2001**, *5*, 724−735. (g) Shaik, S.; Kumar, D.; de Visser, S. P.; Ahmet, A.; Thiel. W. *Chem. Rev.* **2005**, *105*, 2279−2328.

(4) (a) Kumar, D.; Derat, E.; Khenkin, A. M.; Neumann, R.; Shaik, S. *J. Am. Chem. Soc.* **2005**, *127*, 17712−17718. (b) de Visser, S. P.; Kumar, D.; Neumann, R.; Shaik, S. *Angew. Chem., Int. Ed.* **2004**, *43*, 5661−5665.

(5) (a) Groves, J. T.; Stern, M. K. *J. Am. Chem. Soc.* **1984**, *109*, 3812−3814. (b) Arasasingham, R. D.; He, G. X.; Bruice, T. C. *J. Am. Chem. Soc.* **1993**, *115*, 7985−7991. (c) Groves, J. T.; Lee, J.; Marla, S. S. *J. Am. Chem. Soc.* **1997**, *119*, 6269−6273. (d) Zhang, R.; Newcomb, M. *J. Am. Chem. Soc.* **2003**, *125*, 12418−12419. (e) Zhang, R.; Horner, J. H.; Newcomb, M. *J. Am. Chem. Soc.* **2005**, *127*, 6573−6582. (f) Zhang, R.; Harischandra, D. N.; Newcomb, M. *Chem.—Eur. J.* **2005**, *11*, 5713−5720.

(6) (a) Feichtinger, D.; Plattner, D. A. *Angew. Chem., Int. Ed. Engl.* **1997**, *36*, 1718−1719. (b) Feichtinger, D.; Plattner, D. A. *Perkin 2* **2000**, 1023−1028. (d) Li, Z.; Tang, Z. H.; Hu, X. X.; Xia, C. G. *Chem.—Eur. J.* **2005**, *11*, 1210−1216. (d) Khavrutskii, I. V.; Musaev, D. G.; Morokuma, K. *Inorg. Chem.* **2005**, *44*, 306−315.

(7) (a) Gross, Z.; Golubkov, G.; Simkhovich, L. *Angew. Chem., Int. Ed.* **2000**, *39*, 4045−4047. (b) Wang, S. H.; Mandimutsira, B. S.; Todd, R.; Randhanie, B.; Fox, J. P.; Goldberg, D. P. *J. Am. Chem. Soc.* **2004**, *126*, 18−19.

(8) (a) Mandimutsira, B. S.; Randhanie, B.; Todd, R. C.; Wang, H.; Zareba, A. A.; Czernuszewicz, R. S.; Goldberg, D. P. *J. Am. Chem. Soc.* **2002**, *124*, 15170−15171. (b) Lansky, D. E.; Mandimutsira, B.; Ramdhanie, B.; Clausen, M.; Penner-Hahn, J.; Zvyagin, S. A.; Telser, J.; Krzystek, J.; Zhan, R.; Ou, Z.; Kadish, K. M.; Zakharov, L.; Rheingold, A. L.; Goldberg, D. P. *Inorg. Chem.* **2005**, *44*, 4485−4498.

(9) (a) Collins, T. J.; Powell, R. D.; Slebodnick, C.; Ufellman, E. S. *J. Am. Chem. Soc.* **1990**, *112*, 899−901. (b) Collins, T. J.; Gordon-Wylie, S. W. *J. Am. Chem. Soc.* **1989**, *111*, 4511−4513. (c) Workman, J. M.; Powell, R. D.; Procyk, A. D.; Collins, T. J.; Bocian, D. F. *Inorg. Chem.* **1992**, *31*, 1548−1550. (d) Gilbert, B. C.; Kamp, N. W. J.; Lindsay-Smith, J. R.; Oakes, J. *J. Chem. Soc., Perkin. Trans. 2* **1998**, 1841−1844.

(10) (a) Zhang, X. Y.; Pope, M. T. *J. Mol. Catal. A* **1996**, *114*, 201−208. (b) Zhang, X.-Y.; Jameson, G. B.; O'Connor, C. J.; Pope, M. T. *Polyhedron* **1996**, *15*, 917−922. (c) Zhang, X.-Y.; O'Connor, C. J.; Jameson, G. B.; Pope, Michael T. *Inorg. Chem.* **1996**, *35*, 30−34. (d) Zhang, X. Y.; Pope, M. T.; Chance, M. R.; Jameson, G. B. *Polyhedron* **1995**, *14*, 1381−1392.

Table 1. Catalytic Oxidation of Organic Compounds by $F_5PhI(TFAc)_2$ Catalyzed by $P_2W_{17}Mn^{III}$ [a]

substrate	products	yield, mol %
cyclooctene	cyclooctene oxide	80
cyclohexene	cyclohexene oxide (16%), cyclohexenol (58%), cyclohexenone (26%)	56
1-octene	1-octene oxide	56
trans-2-octene	*trans*-2-octene oxide	53
cis-stilbene	*cis*-stilbene oxide (74%), *trans*-stilbene oxide (26%)	19
trans-stilbene	*trans*-stilbene oxide	16
thioanisole	methyl phenyl sulfoxide	86
thianthrene oxide	thianthrene disulfoxide (51%), thianthrene dioxide (49%)	59
cyclohexane	cyclohexanol (43%), cyclohexanone (57%)	18

[a] Reaction conditions: 1 M substrate, 0.064 M $F_5PhI(TFAc)_2$, 0.002 M $P_2W_{17}Mn^{III}$, in 1:1 dichloromethane/acetonitrile under argon, T = room temperature, t = 30 min. The yield is based on $F_5PhI(TFAc)_2$ consumed (~100%). The products noted are the only ones observed resulting from the given substrate. No solvent-related products were observed. Control reactions without $P_2W_{17}Mn^{III}$ on two reactive substrates, cyclooctene and *cis*-stilbene, revealed that comparable yields were obtained after 48 and 96 h, respectively, whereas less reactive substrates such as 1-octene and cyclohexane showed only traces of product after 1 week.

epoxidation of alkenes showed yields comparable to those described for $P_2W_{17}Mn^{III}$/PhIO;[1b] however, the reaction selectivity was somewhat different. Substrates such as 1-octene, *trans*-2-octene, and cyclooctene with stronger allylic C−H bonds gave epoxides as the only observable product. On the other hand, cyclohexene with a weaker allylic C−H bond was preferably hydroxylated rather than epoxidized. $P_2W_{17}Mn^{III}$/PhIO exhibited much more selective epoxidation in the oxidation of cyclohexene.[1b] *cis*- and *trans*-stilbene were similarly reactive; no significant isomerization of *cis*- to *trans*-stilbene was observed, and more importantly, the reaction was reasonably stereoselective. $P_2W_{17}Mn^{III}$/PhIO showed differences in the reactivity of *cis*- and *trans*-stilbene and was less stereoselective.[1b]

An important further observation in oxidations catalyzed by $P_2W_{17}Mn^{III}/F_5PhI(TFAc)_2$ was that upon addition of $F_5PhI(TFAc)_2$ to a 2 mM pink solution of $P_2W_{17}Mn^{III}$, a green solution was obtained with or without a substrate such as cyclooctene, 1-octene, or thioanisole in 1:1 dichloromethane/acetonitrile. The solution remained green until the $F_5PhI(TFAc)_2$ oxidant was consumed, whereupon the pink color returned. The related UV−vis spectra are shown in Figure 2.

One may observe that the original starting compound has a clear peak at λ_{max} = 476 nm (ϵ = 2500 M^{-1} cm^{-1}). Upon addition of 1 equiv of $F_5PhI(TFAc)_2$ to the 0.04 mM solution of $P_2W_{17}Mn^{III}$, the solution immediately turns green with a more intense spectrum throughout the 400−700 nm region with no maximum. After 600 s the emerging reappearance of the original $P_2W_{17}Mn^{III}$ spectrum may be observed (the spectrum is vertically offset for improved visualization). If excess substrate, such as 1-octene, is added, then the original spectrum of $P_2W_{17}Mn^{III}$ is observable after 600 s. The described UV−vis experiment indicated the presence of an observable intermediate and led to further study on the nature of the active species.

First, using ^{19}F NMR, we sought to understand the reaction and fate of the $F_5PhI(TFAc)_2$ oxidant in the presence of $P_2W_{17}Mn^{III}$, Figure 3. $F_5PhI(TFAc)_2$ (bottom spectrum) shows peaks at −119.5, −138.7, and −153.8 ppm, marked "s", attributable to the *m*-, *p*-, and *o*-fluorine atoms, respectively. An additional peak for the trifluoroacetate moiety (not shown) appears at −73.0 ppm. Upon addition of $P_2W_{17}Mn^{III}$ at −50 °C (middle spectrum) six additional peaks were observed.

After allowing the solution warm to −20 °C (top spectrum), only three peaks are observed at −119.23, −152.19, and −159.34 ppm, marked "p", attributable also by measurement of a reference standard to the *m*-, *p*-, and *o*-fluorine atoms, respectively, of the pentafluoroiodobenzene (F_5PhI) product. An additional peak for the free trifluoracetic acid (not shown) appears at −75.7 ppm. Thus, the three additional peaks observed

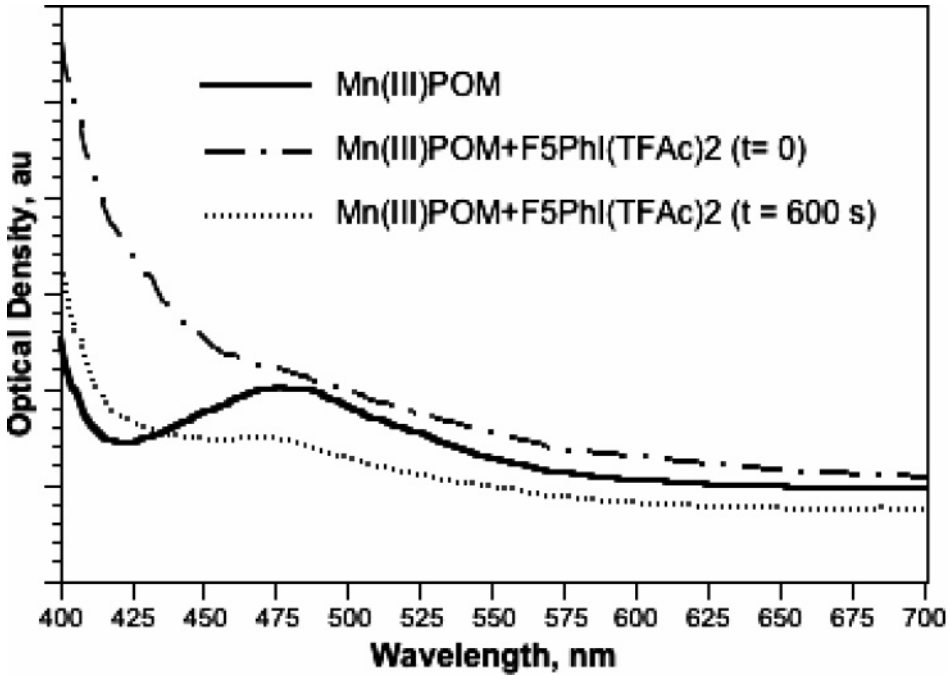

Figure 2. Spectra of $P_2W_{17}Mn^{III}$ before and after addition of $F_5PhI(TFAc)_2$. Measurement conditions: the UV−vis spectrum of a 0.04 mM solution of $P_2W_{17}Mn^{III}$ was measured at 25 °C followed by addition of 1 equiv of $F_5PhI(TFAc)_2$ and measurement at 5 s intervals.

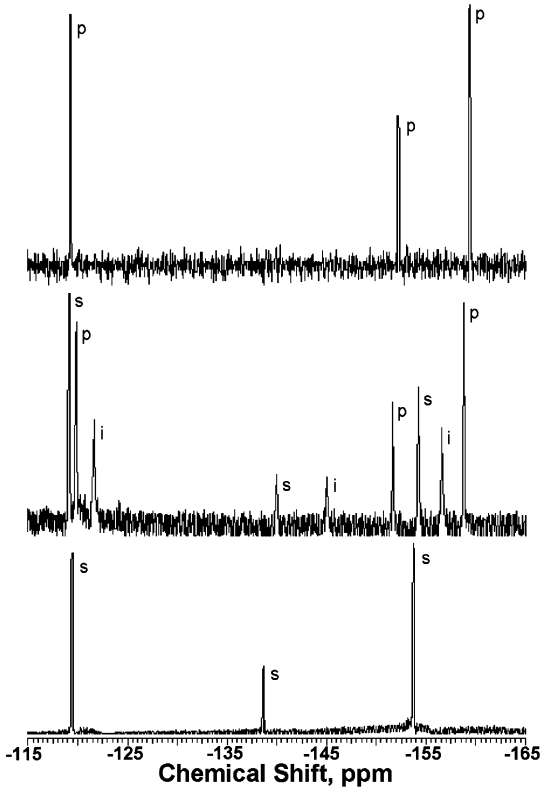

Figure 3. ^{19}F NMR spectra of $F_5PhI(TFAc)_2$ (bottom), after addition of $P_2W_{17}Mn^{III}$ at −50 °C (middle), and after warming to −20 °C (top). Measurement conditions: $F_5PhI(TFAc)_2$ was dissolved in 1:1 CH_2Cl_2/CD_3CN and cooled to −78 °C, after which 5 equiv of $P_2W_{17}Mn^{III}$ was added. The spectra were measured first at −50 °C and then at −20 °C.

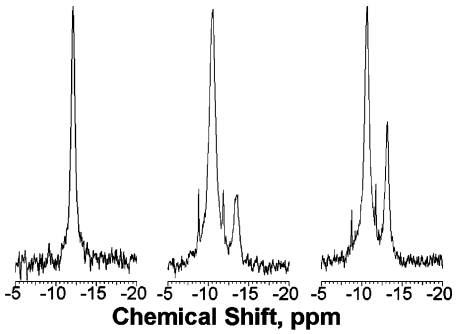

Figure 4. ^{31}P NMR spectra of $P_2W_{17}Mn^{III}$ (left), after addition of $F_5PhI(TFAc)_2$ at −50 °C (middle), and after warming to −20 °C (right). Measurement conditions: $P_2W_{17}Mn^{III}$ was dissolved in 1:1 CH_2Cl_2/CD_3CN and cooled to −78 °C, after which 5 equiv of $F_5PhI(TFAc)_2$ was added. The spectra were measured first at −50 °C and then at −20 °C.

at −50 °C, not associated with either $F_5PhI(TFAc)_2$ or F_5PhI, and appearing at −121.7, −145.0, and −156.6 ppm, marked "i", are attributable to an intermediate complex, $F_5PhIO-P_2W_{17}Mn^{III}$. It should be noted that the peaks of $F_5PhI(TFAc)_2$ and F_5PhI appear at slightly different chemical shifts in the various spectra. This is due to the different measurement temperatures and the different paramagnetism of each solution. Importantly, already at −50 °C the $F_5PhIO-P_2W_{17}Mn^{III}$ intermediate decomposes significantly; this is in contrast to the situation using an iron(III)-substituted polyoxometalate where such an intermediate remained stable for a lengthy period of time and very little free F_5PhI was formed even at room temperature.[4a]

It is also very notable that the green compound formed by addition of $F_5PhI(TFAc)_2$ to $P_2W_{17}Mn^{III}$ at room temperature and then quenched to −50 °C showed no evidence of the intermediate species, indicating that the green compound is not $P_2W_{17}Mn^{III}$ but rather a suggested Mn(V)═O-substituted polyoxometalate ($P_2W_{17}Mn^{V}$═O), Scheme 1. Additionally, the solution of the species formed at −50 °C remains green at −20 °C (and even for some time at room temperature), indicating that the disappearance of the intermediate $F_5PhIO-P_2W_{17}Mn^{III}$ is not associated with re-formation of the initial Mn(III) compound.

To obtain further evidence for $P_2W_{17}Mn^{V}$═O, we carried out an additional ^{31}P NMR experiment, Figure 4, utilizing the fact that the two phosphorus atoms in $P_2W_{17}Mn^{III}$ are in different chemical environments. The spectrum of the original Mn(III)-substituted polyoxometalate (Figure 4, left) shows a broad singlet at −12.8 ppm attributable to the phosphorus atom distal to the paramagnetic Mn(III) center. The peak for the phosphorus atom proximal to Mn(III) was expectedly not observed. After addition of $F_5PhI(TFAc)_2$ to $P_2W_{17}Mn^{III}$ at −50 °C (Figure 4, middle), a considerably different spectrum is observed; broad peaks are observable at −10.6 and −13.2 ppm, and narrow peaks are observed at −8.8 and −11.9 ppm. This spectrum remains mostly unchanged even upon warming to −20 °C (Figure 4, right).

Considering first the spectrum measured at −50 °C and according to our hypothesis presented in Scheme 1, based on the UV−vis and ^{19}F NMR experiments, the solution should contain the proposed $P_2W_{17}Mn^{V}$═O species, the $F_5PhIO-P_2W_{17}Mn^{III}$ intermediate, and some of the initial $P_2W_{17}Mn^{III}$ polyoxometalate. Taking into account temperature effects and paramagnetic effects of other species, the broad peak at −13.2 ppm can be reasonably assigned to the initial $P_2W_{17}Mn^{III}$ polyoxometalate. The $F_5PhIO-P_2W_{17}Mn^{III}$ species is necessarily paramagnetic (d^4) and therefore should also display a broad singlet for the phosphorus atom distal to the manganese center. It is tempting, therefore, to assign the broad peak at −10.6 ppm to $F_5PhIO-P_2W_{17}Mn^{III}$. On the other hand, the $P_2W_{17}Mn^{V}$═O species (d^2) can be either a low-spin diamagnetic singlet or a high-spin paramagnetic triplet (see the computational results below). The ^{31}P NMR spectrum with two narrow peaks at −8.8 and −11.9 ppm can be clearly associated with the two environmentally different phosphorus atoms in a low-spin $P_2W_{17}Mn^{V}$═O species. In fact, diamagnetic species can be uniquely associated with a low-spin Mn(V) compound.[12] On the other hand, the high-spin triplet $P_2W_{17}Mn^{V}$═O species may also be associated with the broad peak at −10.6 ppm, perhaps overlapping with the peak associated with the $F_5PhIO-P_2W_{17}Mn^{III}$. In fact, by heating the solution to −20 °C (Figure 4, right), conditions under which the ^{19}F NMR showed the disappearance of $F_5PhIO-P_2W_{17}Mn^{III}$, yet which remained green, support is lent to the conclusion that indeed the peak at −10.6 ppm is probably attributable to both $F_5PhIO-P_2W_{17}Mn^{III}$ and high-spin triplet $P_2W_{17}Mn^{V}$═O.

(11) Adam, W.; Haas, W.; Lohray, B. B. *J. Am. Chem. Soc.* **1991**, *113*, 6202−6208.

(12) As a reviewer noted, a diamagnetic species could conceivably also arise from an antiferromagnetically coupled Mn(IV)−O−Mn(IV) dimer. Although this is possible, we observed no EPR signal even down to 6 K. Also, we feel that we can exclude this assignment of the narrow peaks because the diamagnetic species is not persistent in the presence of oxygen acceptors (substrates), although one would expect the opposite for a Mn(IV)−O−Mn(IV) dimer; it should be quite stable in solution. Furthermore, one would expect the Mn(IV)−O−Mn(IV) dimer to be a poor oxygen donor especially since it has already been shown that even monomeric Mn(IV)−O species are not reactive (ref 10).

Scheme 1. Reaction of $P_2W_{17}Mn^{III}$ with $F_5PhI(TFAc)_2$

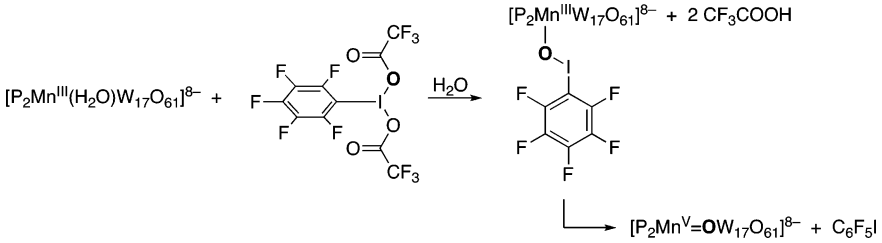

The combined experimental results using UV−vis and ^{19}F and ^{31}P NMR indicate that the addition of $F_5PhI(TFAc)_2$ to $P_2W_{17}Mn^{III}$ leads to formation of an active $P_2W_{17}Mn^{V}$═O species responsible for the catalytic activity of the manganese-substituted polyoxometalate; this active species should have a diamagnetic ground state with a closely lying triplet state. The competency of the proposed $P_2W_{17}Mn^{V}$═O species as an oxidant was also tested in stoichiometric reactions. Thus, $P_2W_{17}Mn^{V}$═O was prepared by addition of 15 μmol of $F_5PhI(TFAc)_2$ in 0.5 mL of 1:1 CH_2Cl_2/CH_3CN to 10 μmol of $P_2W_{17}Mn^{III}$ dissolved in 0.5 mL of 1:1 CH_2Cl_2/CH_3CN at −45 °C. The solution was heated to −20 °C, yielding the "green compound", and 50 mmol of substrate was added. The reaction mixture was kept at −20 °C until the solution turned pink and then was analyzed by GC and GC−MS. The results for the oxidation of several substrates are as follows (yield based on $P_2W_{17}Mn^{III}$): (i) cyclohexene (yield 48%), cyclohexene oxide (13%), cyclohexenol (87%), (ii) *cis*-stilbene (yield 23%), *cis*-stilbene oxide (78%), *trans*-stibene oxide (22%), (iii) thioanisole (yield 85%), methyl phenyl sulfoxide (100%). The results show that the proposed $P_2W_{17}Mn^{V}$═O species is a competent oxygen donor. Furthermore, the reaction selectivities observed in stoichiometric reactions for cyclohexene oxidation (epoxidation versus allylic oxidation), *cis*-stilbene epoxidation (ratio of *cis*-epoxide to *trans*-epoxide), and thioanisole oxidation (exclusive formation of sulfoxide) are very similar to the selectivities observed in the catalytic reactions (Table 1). This also supports the notion that $P_2W_{17}Mn^{V}$═O is the reactive species and that the F_5PhIO−$P_2W_{17}Mn^{III}$ intermediate is not involved in oxygen transfer.

It is also worth noting that the epoxidation of *trans*-stilbene (0.5 M substrate, 0.9 M $H_2{}^{18}O$ (94.3% ^{18}O labeled), 0.064 M $F_5PhI(TFAc)_2$, 0.002 M $P_2W_{17}Mn^{III}$ in 1:1 dichloromethane/acetonitrile under argon, T = room temperature, t = 30 m) led to 68% incorporation of ^{18}O into *trans*-stilbene oxide, while addition of $H_2{}^{18}O$ to preformed *trans*-stilbene oxide, also in the presence of $P_2W_{17}Mn^{III}$, did not lead to ^{18}O incorporation. This high ^{18}O incorporation indicates exchange of the active oxygen facilitated by its coordination to the manganese center and supports the reaction pathway presented in Scheme 1.[13]

To gain insight into the electronic structure and reactivity of the proposed $P_2W_{17}Mn^{V}$═O species, we further studied a Mn^{V}═O-containing polyoxometalate by means of density functional theory (DFT) using the similar Keggin analogue as a model (Figure 1, left). The relevant $[PW_{11}O_{39}Mn^{V}$═$O]^{4-}$ species was generated from the parent $[PW_{12}O_{40}]^{3-}$, for which there is excellent neutron diffraction structural data,[14] by replacing a single W^{VI}═O moiety with Mn^{V}═O. This was followed by full and unconstrained optimization of the structure and verification that it is a minimum by means of frequency calculations. Thus, the resulting optimized structure for the $[PW_{11}O_{39}Mn^{V}$═$O]^{4-}$ complex exhibits a Mn^{V}═O moiety coordinated to four oxygen atoms (O_b) on the surface of the polyoxometalate and to one axial oxygen atom (O_i), which is part of the central phosphate (see Figure 1, left). With this distorted hexacoordination, the five d-block orbitals spread into $\delta + 2\pi^* + 2\sigma^*$ orbitals, where the asterisk signifies antibonding interaction with the ligands, Figure 5. Importantly, in the case of π^* the antibonding interaction is mostly across the Mn═O linkage.[4] In addition, there is a high-lying lone-pair orbital (lp) that lies close to these d orbitals.[4] We have calculated, therefore, a closed shell singlet with a δ^2 configuration and a triplet with a $\delta^1\pi^{*1}$ configuration, along with its corresponding open-shell $\delta^1\pi^{*1}$ singlet (for other states, see the Supporting Information, SI). The key optimized bond lengths for $[PW_{11}O_{39}Mn^{V}$═$O]^{4-}$ are summarized in Table 2. The most notable difference is along the O_t−Mn−O axis. The Mn═O bond is particularly shorter and the O_t−Mn bond

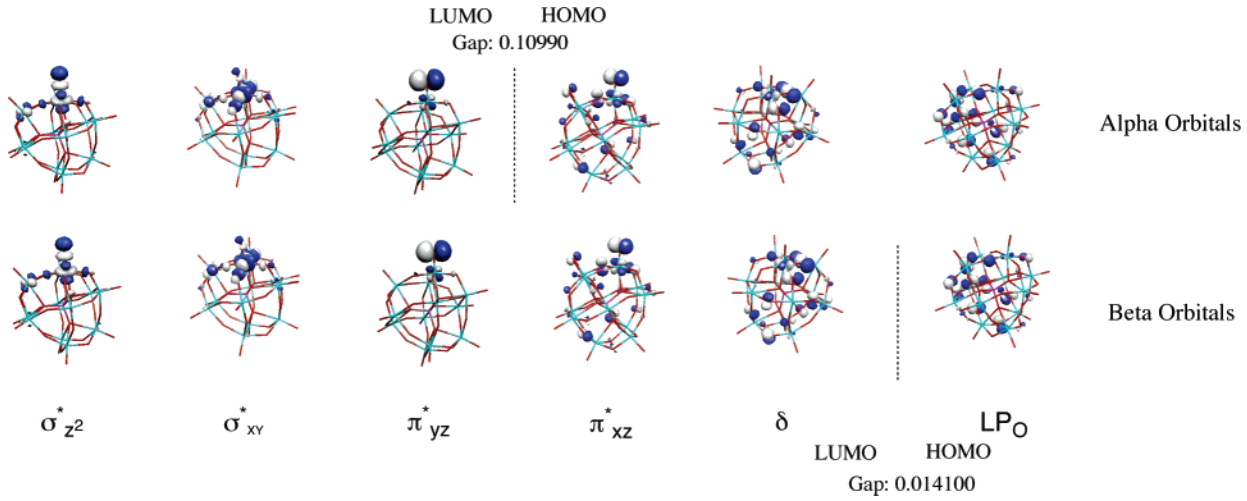

Figure 5. Molecular orbitals of $[PW_{11}O_{39}Mn^{V}$═$O]^{4-}$.

Table 2. UB3LYP/B1-Optimized Key Bond Lengths of $[PW_{11}O_{39}Mn^{V}{=}O]^{4-}$ in the Singlet (δ^2 Configuration) and Triplet States

bond	singlet bond length, Å	triplet bond length, Å	bond	singlet bond length, Å	triplet bond length, Å
Mn−O	1.571	1.751	W−O_b	1.857	1.862
Mn−O_b	1.871	1.883	W−O_t	1.743	1.733
Mn−O_i	2.350	2.138			

Table 3. Relative Energies (kcal/mol) for the Three Spin States of $[PW_{11}O_{39}Mn^{V}{=}O]^{4-}$

	UB3LYP			UBLYP		
spin state	gas phase	$\epsilon = 5.7$	$\epsilon = 37.5$	gas phase	$\epsilon = 5.7$	$\epsilon = 37.5$
$\delta^1\pi^{*1}\,{}^1\mathbf{1}'$	0.4	0.7	0.8	1.4	1.5	1.5
$\delta^2\,{}^1\mathbf{1}$	0.0	0.0	0.0	0.0	0.0	0.0
$\delta^1\pi^{*1}\,{}^3\mathbf{1}$	−16.0	−14.8	−15.0	0.1	1.1	1.1

is thus longer for the closed shell singlet, in which the antibonding Mn−O orbitals are vacant. The Mn═O bond gets longer as more of these antibonding orbitals are populated; note that a similar observation was made by Groves et al.[17b] This short Mn═O bond in the singlet state results in large barriers for oxidations through this state (see below) and hence in reactivity via different spin states. For bond lengths not presented in Table 2 there were no significant differences between the singlet and triplet states.

Previously we have shown that for the corresponding oxoiron species $[PW_{11}O_{39}Fe{=}O]^{4-}$, both UB3LYP and the pure functional BP86 gave the same spin-state ordering.[4] However, for manganese complexes,[15] there is still no consensus on the best DFT method for reproducing the correct spin-state ordering. Therefore, we tested alongside UB3LYP a few pure GGA functionals: UBP86,[16a,b] UBLYP,[16b,c] UBPW91,[16a,d] and the modified hybrid functional UB3LYP*.[16e] The UB3LYP* results are similar to those for UB3LYP, while all the pure functionals gave the same ordering of the spin states, which is different from that of B3LYP. Therefore, we show in Table 3 only the results using UB3LYP and UBLYP; the rest of the data can be found in the SI.

It is apparent that using UB3LYP the triplet $\delta^1\pi^{*1}$ state is the ground state with significantly higher lying singlet states, whereas using UBLYP the triplet and singlet states have similar energies. On the basis of the NMR and other data presented above, one can conclude that the pure UBLYP functional more appropriately defines the relative energies of the two lowest spin states for $[PW_{11}O_{39}Mn^{V}{=}O]^{4-}$.[17]

After having probed the geometry and the electronic structure of $[PW_{11}O_{39}Mn^{V}{=}O]^{4-}$, we turned to a study of the reaction pathway for epoxidation and hydroxylation using propene as the substrate, Scheme 2.

To probe the nature of the lowest energy transition state, we calculated the relative energies of the six transition states for bond activation for the different spin states for epoxidation and hydroxylation. The results using the pure and hybrid functionals are shown in Figure 6. It can be seen that for both functionals the singlet and also quintet states are in all likelihood not the reactive states; their transition states are significantly higher in energy than those of the triplet state. The high energy of the singlet transition states can be traced to the short Mn═O bond in the ground state of $[PW_{11}O_{39}Mn^{V}{=}O]^{4-}$, Table 2. Thus, during the bond activation in propene, the Mn═O bond has to stretch and will thereby contribute to the barrier; the shorter the Mn═O bond, the more energy is expended in its stretching and the larger will be the barrier. It follows, therefore, that the high barrier of the singlet state has a clear chemical rationale and is also independent of the functional used for the calculations.

The UBLYP energy profiles for double bond epoxidation and allylic hydroxylation are shown in Figure 7, and the analogous UB3LYP energy profiles can be found in the SI. A few trends are notable: (i) As noted above, the gas-phase barriers on the triplet state are small. (ii) At the B1 level using UBLYP and at the higher B2 level with UB3LYP with solvent correction, the epoxidation process is calculated to be downhill, while the hydroxylation has a tiny barrier for bond activation. The large solvent correction effect is due to the high negative charge of the polyoxometalate that magnifies Born solvation energies since solvation effects are proportional to Q^2 (Q = charge).[4a] Thus, for the reaction complex $Q = 4-$, while at the TS the polyoxometalate cluster acquires a higher negative charge ($Q \approx 4.3-$; see the SI) due to charge transfer from the propene. Since the TS solvation will be proportional to $[Q + \Delta Q]$,[2] it can be shown that, due to this increment of negative charge, the solvation of the TS will be magnified (in proportion to $2(\Delta Q)Q$) relative to the ground state, thereby lowering the reaction barrier significantly. (iii) In both oxidation processes,

Scheme 2. Reaction Pathways Studied for Epoxidation and Hydroxylation of Propene by $[PW_{11}O_{39}Mn^{V}{=}O]^{4-}$ [a]

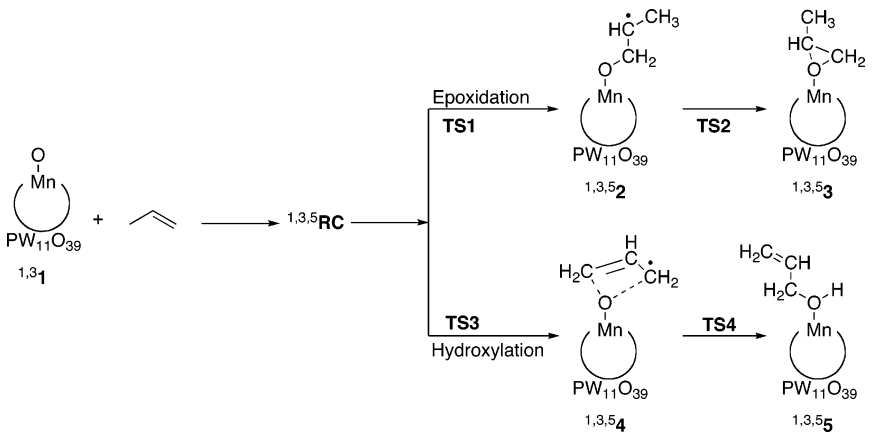

[a] RC = reactive complex, and TS = transition state.

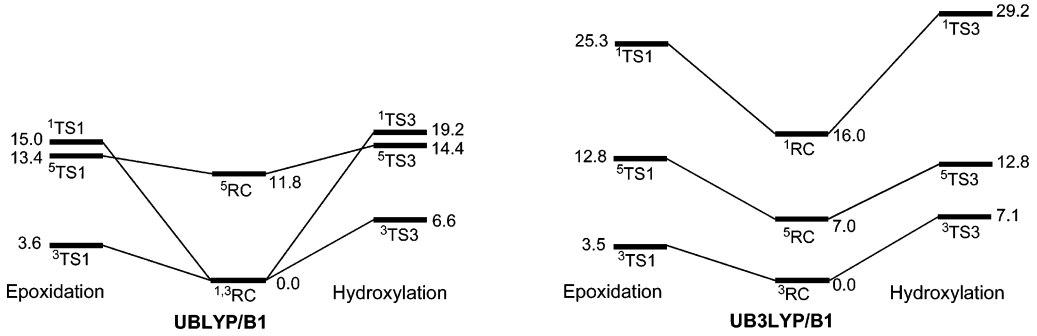

Figure 6. Relative energies (kcal/mol) of bond activation transition states for epoxidation (^{1,3,5}TS1) and hydroxylation (^{1,3,5}TS3).

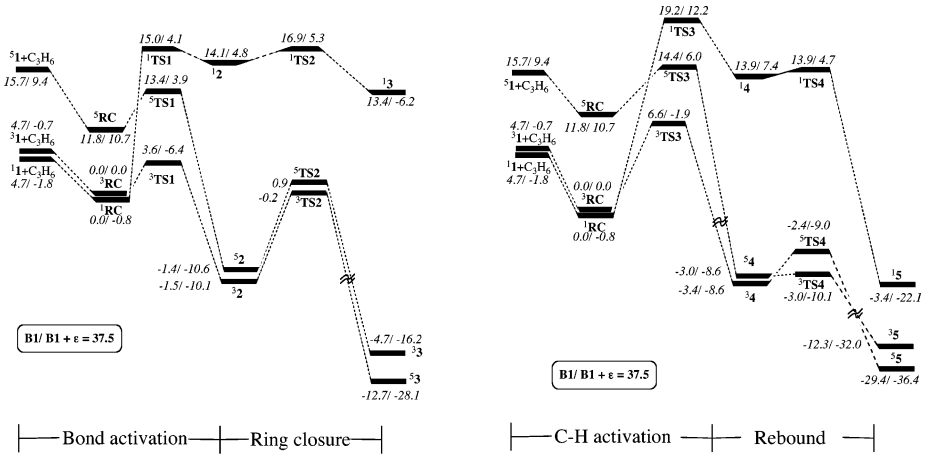

Figure 7. UBLYP energy profile for epoxidation (left) and hydroxylation (right). The energies in each line follow the order indicated in the box.

if the reaction starts at the singlet state, it will have to cross over to the triplet surface; hence, it will show two-state reactivity (TSR).[18] (iv) At the intermediate stage, the quintet intermediate may be sufficiently low lying to participate in the product formation. (v) If the reaction begins at the triplet state, no crossover will be necessary. This scenario of many spin states is somewhat reminiscent of the reactivity of iron−oxo complexes developed by Que and co-workers.[19]

The computations show that $[PW_{11}O_{39}Mn{=}O]^{4-}$ is a very powerful oxidant, a more powerful oxidant than $[PW_{11}O_{39}Fe{=}O]^{4-}$, which we recently computationally investigated.[4a] The rationale for this can be traced to the relative strengths of the Fe=O versus Mn=O bonds that has also been observed in metalloporphyrin species.[17b] As seen in Table 2, the Mn=O bond length in the reactive triplet state is 1.751 Å, while the corresponding Fe=O bond length is 1.667 Å.[4a] Since the TM=O bond itself undergoes activation in the transition state, the stronger bond in $[PW_{11}O_{39}Fe{=}O]^{4-}$ will lead to higher barriers compared with those of $[PW_{11}O_{39}Mn{=}O]^{4-}$, which has a significantly weaker bond. The weaker Mn=O bond must originate in the higher antibonding character of the π^* orbitals of the Mn=O moiety. This bond weakening effect in $[PW_{11}O_{39}Mn{=}O]^{4-}$ versus $[PW_{11}O_{39}Fe{=}O]^{4-}$ is apparent by comparing the exothermicity of the bond activation step for the two reagents.[4a] In each case, hydroxylation or epoxidation, the $[PW_{11}O_{39}Mn{=}O]^{4-}$ process is more exothermic by ca. 10 kcal/mol.

The calculations show that, for propene, epoxidation is the preferred reaction pathway compared to allylic hydroxylation, ^{3}TS3 > ^{3}TS1. This is in concert with the experimental results observed for 1-octene, a reasonable model for propene, which showed only epoxidation and no evidence of allylic hydroxylation. Cyclohexene with weaker allylic C−H bonds (BDE(cyclohexene) = 81.6 kcal/mol,[20a] BDE(propene) = 86.4 kcal/mol[20b]) preferably undergoes allylic hydroxylation; this is also in reasonable agreement with the calculated results that show only a difference of ∼3 kcal/mol for ^{3}TS3 versus ^{3}TS1 in propene.

Furthermore, the calculations show that both POM−TM=O reagents (TM = transition metal) are expected to be more powerful than compound I of cytochrome P450 or any other

(13) (a) Nam, W.; Valentine, J. S. *J. Am. Chem. Soc.* **1993**, *115*, 1772−1778. (b) Groves, J. T.; Kruper, W. J. *J. Am. Chem. Soc.* **1979**, *101*, 7613−7615. (c) Leising, R. A.; Brennan, B. A.; Que, L.; Munck, E. *J. Am. Chem. Soc.* **1991**, *113*, 3988−3990.

(14) Brown, G. M.; Noe-Spirlet, M. R.; Busing, W. R.; Levy, H. A. *Acta Crystallogr., B* **1977**, *34*, 1038−1046.

(15) (a) Ghosh, A.; Persson, B. J.; Taylor, P. R. *J. Biol. Inorg. Chem.* **2003**, *8*, 507−511. (b) Ghosh, A.; Taylor, P. R. *Curr. Opin. Chem. Biol.* **2003**, *7*, 113−124.

(16) (a) Becke, A. D. *Phys. Rev. A* **1988**, *36*, 3098−3100. (b) Perdew, J. P. *Phys. Rev. B* **1986**, *33*, 8822−8824. (c) Li, C.; Yang. W.; Parr, R. G. *Phys. Rev. B* **1998-I**, *37*, 785−789. (d) Perdew, J. P.; Wang, Y. *Phys. Rev. B* **1992**, *45*, 13245−13249. (e) Reiher, M.; Salomon, O.; Hess, B. A. *Theor. Chem. Acc.* **2001,** *107*, 48−55.

(17) (a) It has been noted in the past that while hybrid functionals are usually better than pure functionals, they can show occasionally increased stabilization of high spin states; cf. Salomon, O.; Reiher, M.; Hess, B.A. *J. Chem. Phys.* **2002**, *117*, 4729−4737. Harvey, J. N. *Struct. Bonding* **2004**, *112*, 151−183. Smith, D. M.; Dupuis, M.; Straasma, T. P. *Mol. Phys.* **2005**, *103*, 273−278. (b) The use of a pure functional has also been recently shown to better fit the experimentally observed spin states for a Mn(V)=O porphyrin; cf. De Angelis, F.; Jin, N.; Car, R. Groves, J. T. *Inorg. Chem.* **2006**, *45*, 4268−4276.

(18) (a) Shaik, S; Cohen, S.; de Visser, S. P.; Sharma, P. K.; Kumar, D.; Kozuch, S.; Ogliaro, F; Danovich, D. *Eur. J. Inorg. Chem.* **2004**, *35*, 207−226. (b) Shaik, S.; de Visser, S. P.; Ogliaro, F.; Schwarz, H.; Schröder, D. *Curr. Opin. Chem. Biol.* **2002**, *6*, 556−567. (c) Shaik, S.; Filatov, M.; Schröder, D.; Schwarz, H. *Chem.—Eur. J.* **1998**, *4*, 193. (d) Danovich, D.; Shaik, S. *J. Am. Chem. Soc.* **1997**, *119*, 1773−1786.

oxoiron species computed by us to date.[21] As noted in the past,[4a] the reasons for the higher *calculated* potency of the POM−TM=O reagents can be ascribed to the large anionic charge (4−) of the POM−TM=O species. Since at the bond activation transition states there is some charge transfer from the reagent to the POM−TM=O reagent, the Coulomb interaction between the positively charged substrate ($Q = 0.24-0.29$; see the SI) and the high negative charge of the reagent lowers the barriers already in the gas phase by a considerable amount compared to those of compound I of cytochrome P450, which is a neutral reagent. Furthermore, as noted above, the transition-state solvation energy is amplified relative to that of the ground state, and the barrier is further reduced after solvent correction. In the case of $[PW_{11}O_{39}Fe{=}O]^{4-}$, the barriers remain significant, but in $[PW_{11}O_{39}Mn{=}O]^{4-}$, the barriers virtually vanish.

Of course, the foregoing argument is based on energy only and does not include entropic factors, which may be very significant for the highly charged polyoxometalate reagent. Indeed, the relative barriers obtained in the computational results, showing that $[PW_{11}O_{39}Mn{=}O]^4$ is a stronger oxidant compared to the analogous Mn^V=O porphyrin, has not been substantiated by experiment. In fact, prior to this work, two lines of evidence pointed to the opposite: (i) $P_2W_{17}Mn^V$=O can be trapped and observed quite easily as described herein, whereas the Mn^V=O porphyrin cannot normally be observed since it is too reactive; substitution of the porphine moiety by four cationic pyridyl moieties allowed the observation of Mn^V=O species.[22] (ii) Kinetic measurements carried out under identical conditions showed that manganese(III) tetraphenylporphyrin (Mn^{III}TPP) was a considerably more active catalyst compared to $P_2W_{17}Mn^{III}$ although the actual reactivity of neither the proposed active $P_2W_{17}Mn^V$=O nor Mn^V=OTPP has been measured.[1b] Therefore, using UV−vis spectrometry, we evaluated the kinetic behavior of $P_2W_{17}Mn^V$=O with 1-octene as a substrate. First, the linear dependence of the observed rate constant as a function of the 1-octene concentration was demonstrated by following the disappearance of 0.5 mM green $P_2W_{17}Mn^V$=O (prepared by adding 1 equiv of $F_5PhI(TFAc)_2$ to $P_2W_{17}Mn^{III}$) at 420 nm with various amounts of 1-octene (5−100 mM), Figure 8. The log k_{obs} versus log [1-octene] plot yielded a slope of 1.06 ($r^2 = 0.99$) showing that the disappearance of green $P_2W_{17}Mn^V$=O is first order in 1-octene.

It should be noted that at 1-octene concentrations lower than 5 mM (10:1 1-octene/$P_2W_{17}Mn^V$=O) the rate of self-decay of $P_2W_{17}Mn^V$=O is too fast relative to that with 1-octene to derive an exact second-order rate equation. However, in the presence of 100 equiv of 1-octene, a pseudo-first-order rate equation, $-d[P_2W_{17}Mn^V{=}O]/dt = k[P_2W_{17}Mn^V{=}O]$, gave at 25 °C a pseudo-first-order rate constant, $k = 1.082 \pm 0.026 \times 10^{-2}\ s^{-1}$ with $\tau_{1/2} = 48$ s. By comparison the reported second-order rate constant for oxomanganese(V) tetrakis(*N*-methylpyrid-4-yl)-porphyrin with an active alkene, carbamazepine, was $6.5 \times 10^5\ M^{-1}\ s^{-1}$.[22a] Under pseudo-first-order conditions, the energy of activation (measured between 7 and 27 °C) was found to be $E_a = 4.32 \pm 0.07$ kcal/mol, Figure 9.

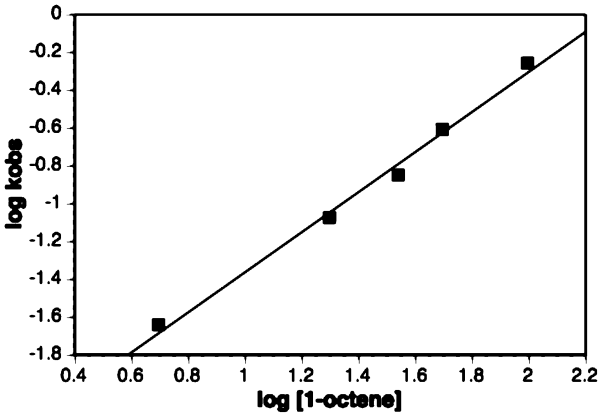

Figure 8. log/log plot of the observed rate of disappearance of $P_2W_{17}Mn^V$=O as a function of the initial concentration of 1-octene (0.5 mM $P_2W_{17}Mn^V$=O from 1:1 $P_2W_{17}Mn^{III}/F_5PhI(TFAc)_2$, 5−50 mM 1-octene in 1:1 CH_2Cl_2/CH_3CN at 25 °C).

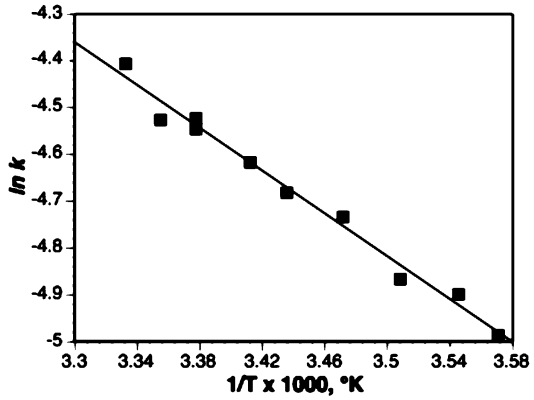

Figure 9. Arrhenius plot for the epoxidation of 1-octene (0.5 mM $P_2W_{17}Mn^V$=O from 1:1 $P_2W_{17}Mn^{III}/F_5PhI(TFAc)_2$, 50 mM 1-octene in 1:1 CH_2Cl_2/CH_3CN).

From the plot presented in Figure 9 the computed values for the enthalpy, entropy, and free energy of activation were calculated: $\Delta H^{\ddagger}_{298} = 3.72 \pm 0.07$ kcal mol^{-1}, $\Delta S^{\ddagger}_{298} = -52.6 \pm 0.4$ cal mol^{-1} K^{-1}, and $\Delta G^{\ddagger}_{298} = 19.4 \pm 0.1$ kcal mol^{-1}. These measurements indicate that experimentally the proposed $P_2W_{17}Mn^V$=O complex indeed has a low barrier ($\Delta H^{\ddagger}_{298} = 3.72$ kcal mol^{-1}) for oxygen transfer in an epoxidation reaction that is in general qualitative agreement with the calculated barrier. Since there are as yet no reports for such measurements for an analogous Mn^V=O porphyrin, a direct comparison with $P_2W_{17}Mn^V$=O is not possible at this stage. However, it is clear considering the rate constants measured herein for $P_2W_{17}Mn^V$=O and the literature reports on the reactivity of oxomanganese(V) tetrakis(*N*-methylpyrid-4-yl)porphyrin[22a] that $P_2W_{17}Mn^V$=O experimentally is in fact a less effective oxygen-transfer agent. The key to understanding the relatively sluggish reactivity of $P_2W_{17}Mn^V$=O probably is connected to the highly negative entropy of activation that was obtained from the experiment in our work ($\Delta S^{\ddagger}_{298} = -52.6$ cal mol^{-1} K^{-1}) and the resulting high free energy of activation ($\Delta G^{\ddagger}_{298} = 19.4$ kcal mol^{-1}). It appears reasonable that the higher charge of TS1 due to charge transfer from the substrate to the polyoxometalate versus the initial polyoxometalate leads to *increased* solvation of TS1 by the polar solvent molecules (acetonitrile) used in the experiment and adventitious water that is surely present in solution. This

(19) Kumar, D.; Hirao, H.; Que, L.; Shaik, S. *J. Am. Chem. Soc.* **2005**, *127*, 8026−8027.
(20) (a) Bryant, J. R.; Mayer, J. M. *J. Am. Chem. Soc.* **2003**, *125*, 10351−10361. (b) Lide, D. R., Ed. *Handbook of Chemistry and Physics*; CRC Press: Boca Raton, FL, 1997; pp 9−64.
(21) (a) de Visser, S. P.; Ogliaro, F.; Sharma, P. K.; Shaik, S. *J. Am. Chem. Soc.* **2002**, *124*, 11809−11826. (b) See ref 3g.
(22) (a) Groves, J. T.; Lee, J.; Marla, S. S. *J. Am. Chem. Soc.* **1997**, *119*, 6269−6270. (b) Jin, N.; Groves, J. T. *J. Am Chem. Soc.* **1999**, *121*, 2923−2924.

causes electrostriction of the solvent and a loss of many degrees of freedom, thereby leading to a high negative entropy of activation and an experimentally high free energy of activation.

Although the computational model takes into account solvent effects, it does so by simulating the dielectric constant without actually including solvent shells in the model reaction pathway (Scheme 2). Ideally and especially when considering highly charged species such as polyoxometalates, such solvent shells should be included in the computational model to attain realistic results in terms of free energies; this will still require a considerable increase in the power of computational techniques for molecules such as large polyoxometalates.

Conclusions

Using UV−vis, ^{19}F NMR, and ^{31}P NMR spectroscopy, we have identified a "green" manganese(V)−oxo intermediate active species, $P_2W_{17}Mn^{V}$═O, formed by the addition of F_5-PhI(TFAc)$_2$ to $P_2W_{17}Mn^{III}$. The ^{31}P NMR spectral assignments indicate that the $P_2W_{17}Mn^{V}$═O species may have both singlet and triplet ground states. Calculation of the electronic structure of $P_2W_{17}Mn^{V}$═O by DFT using the analogous Keggin substituted $[PMn^{V}{=}OW_{11}O_{39}]^{4-}$ confirmed the spectral assignments when using the UBLYP pure functional, while the UB3LYP hybrid functional gave an apparently incorrect ordering of the electronic structures of the ground state. Calculation of energy profiles for the epoxidation and allylic hydroxylation of propene with $[PMn^{V}{=}OW_{11}O_{39}]^{4-}$ showed lowest triplet transition states for both transformations independent of the functional used in the calculation. The calculations predict very low energy barriers for epoxidation of propene, which are expected to be even lower than those for analogous manganese(V)−oxo porphyrins. However, an experimental reaction, the epoxidation of 1-octene by $P_2W_{17}Mn^{V}$═O, measured by UV−vis only partially supports this prediction. Thus, while the enthalpy of activation was indeed low, the very high negative entropy of activation generates a high free energy of activation. The unusually negative entropy of activation that was measured is explained by the increased solvation of the transition state that has a higher polyoxometalate charge than the ground state. The high negative charge of the polyoxometalates renders them very sensitive to solvent effects.

Experimental and Theoretical Methods

Oxidation Reactions. Reactions were carried out in 5 mL vials equipped with a septum and a stirring bar. The catalyst $P_2W_{17}Mn^{III}$, prepared using a known literature method,[23] and substrates were dissolved in a CH_2Cl_2/CH_3CN (1:1) mixture, and the solution was saturated with argon. $F_5PhI(TFAc)_2$ dissolved in solvent was added to initiate the reaction. Typical reaction conditions were 1 M substrate, 0.064 M $F_5PhI(TFAc)_2$, 0.002 M $P_2W_{17}Mn^{III}$, in 1:1 dichloromethane/acetonitrile under argon, T = room temperature, and t = 30 min. GLC analysis was performed on an aliquot withdrawn directly from the reaction mixture after addition of a reference standard to the mixture (usually dodecane). The products were identified using reference standards and or GC−MS measurements. GC and GC−MS measurements were recorded on HP 6890 (FID detector) and HP 5973 (MS detector) instruments equipped with 5% phenyl methyl silicone, 0.32 mm i.d., 0.25 μm coating, 30 m columns (Restek 5MS) using helium as the eluant.

^{19}F NMR Measurements. The samples for low-temperature measurements were prepared as follows: $F_5PhI(TFAc)_2$ was dissolved in 1:1 CH_2Cl_2/CD_3CN and cooled to −78 °C, after which 5 equiv of $P_2W_{17}Mn^{III}$ was added. The spectra were measured first at −50 °C and then at −20 °C. ^{19}F NMR spectra (376.47 MHz, C_6F_6 external standard) were taken on a Bruker Avance 400 instrument.

^{31}P NMR Measurements. The samples for low-temperature measurements were prepared as follows: $P_2W_{17}Mn^{III}$ was dissolved in 1:1 CH_2Cl_2/CD_3CN and cooled to −78 °C, after which 5 equiv of $F_5PhI(TFAc)_2$ was added. The spectra were measured first at −50 °C and then at −20 °C. ^{31}P NMR spectra (161.97 MHz, 85% H_3PO_4 external standard) were taken on a Bruker Avance 400 instrument.

Rate Measurements. UV−vis spectra were taken at 7−27 °C on an HP 8453 diode array spectrometer equipped with a Unisoko UP-1000 cooling system for temperature equilibration. Temperature-dependent measurements were carried out by mixing 2 mL of a 0.5 mM solution of $P_2W_{17}Mn^{III}$ in 1:1 CH_2Cl_2/CH_3CN with 100 equiv of 1-octene that was temperature equilibrated for 10 min in the UV−vis spectrometer with magnetic stirring at 700 rpm. The reaction was initiated by addition of 1 equiv of $F_5PhI(TFAc)_2$ dissolved in 10 mL of 1:1 CH_2Cl_2/CH_3CN, and the UV−vis spectra were then collected every 10 s. Each rate measurement was repeated two or three times. The rate of disappearance of $P_2W_{17}Mn^{V}$═O was measured at 420 nm, where the absorbance of $P_2W_{17}Mn^{III}$ is at a minimum (see Figure 2). The pseudo-first-order rate constants (k_{obs}) were obtained by fitting a plot of $A_{420\,nm}$ versus time to the equation $A_t = A_0e^{-kt}$, where A_t is the absorbance at any given time and A_0 = initial absorbance, both at 420 nm. The decrease in absorbance followed the exponential law for at least 3 half-lives in all cases. Compared to the rate of 100:1 1-octene/$P_2W_{17}Mn^{V}$═O at 25 °C, in the absence of 1-octene, $P_2W_{17}Mn^{V}$═O disappeared at a rate that was about 20 times slower.

Computational Methods. The starting geometry was the neutron diffraction structure[14] of $[PW_{12}O_{40}]^{3-}$ into which the Mn═O moiety was inserted. The resulting structure was optimized by DFT using the unrestricted hybrid functional UB3LYP,[24] combined with the double-ζ effective core potential basis set, LACVP,[25] implemented in JAGUAR 5.5[26] and referred to as B1. All the geometries were optimized with JAGUAR 5.5 without any geometry constraints. The spin states of $[PW_{11}O_{39}Mn{=}O]^{4-}$ and the transition-state structures were verified by frequency calculations, using GAUSSIAN03 (at the UB3LYP/LACVP level),[27] which has a more robust and faster frequency calculation routine. Since frequency calculations for these systems take an extremely long time, the rest of the frequency calculation had to be waived. Reaction pathways, of epoxidation and hydroxylation, as depicted in Scheme 2, were verified by a scan along a given coordinate, while optimizing freely all other coordinates. To test the predictions of UB3LYP, we carried out single-point calculations with a variety of functionals, such as UB3LYP*, and pure functionals,[16] such as UBP86, UBLYP, etc; all these tests were done with B1. Since only the pure functionals predicted the correct ground state for $[PW_{11}O_{39}Mn{=}O]^{4-}$, we describe in the text mostly the results of UBLYP. Nevertheless, as we noted in the Results and Discussion, both UB3LYP and UBLYP show that the singlet state of the reagent is not the reactive state. Indeed, B3LYP is generally useful for polyoxometalate calculations,[4,28] but for some reason is less good for high-valent manganese complexes.[16b]

(23) Lyon, D. K.; Miller, W. K.; Novet, T.; Domaille, P. J.; Evitt, E.; Johnson, D. C.; Finke, R. G. *J. Am. Chem. Soc.* **1991**, *113*, 7209−7221.

(24) (a) Becke, A. D. *J. Chem. Phys.* **1992**, *96*, 2155−2160. (b) Becke, A. D. *J. Chem. Phys.* **1992**, *97*, 9173−9177. (c) Becke, A. D. *J. Chem. Phys.* **1993**, *98*, 5648−5652. (d) Lee, C.; Yang, W.; Parr, R. G. *Phys. Rev. B* **1988**, *37*, 785−789.

(25) LACVP is derived from LANL2DZ; see: Dunning, T. H., Jr.; Hay, P. J. In *Modern Theoretical Chemistry*; Schaefer, H. F., III, Ed.; Plenum: New York, 1976; pp 1−28.

(26) *Jaguar 5.5*; Schrödinger, Inc.: Portland, OR, 2003.

(27) Frisch, M. J.; et al. *Gaussian 03*, Revision C.02; Gaussian, Inc.: Wallingford, CT, 2004.

(28) See for example: (a) Quinonero, D.; Wang, Y.; Morokuma, K.; Khavrutskii, L. A.; Botar, B.; Geletti, Y. V.; Hill, C. L.; Musaev, D. G. *J. Phys. Chem. B* **2006**, *110*, 170−173. (b) Musaev, D. G.; Morokuma, K.; Geletii, Y. V.; Hill, C. L *Inorg. Chem.* **2004**, *43*, 7702−7708. (c) For, a recent interplay of DFT and experiment, see: Anderson, T. M.; Neiwert, W. A.; Kirk, M. L.; Piccoli, P. M. B.; Schultz, A. J.; Koetzle, T. E.; Musaev, D. G.; Morokuma, K.; Cao, R.; Hill, C. L. *Science* **2004**, *306*, 2074−2077.

The energies of all optimized structures were further corrected using single-point calculations with the larger basis set, LACV3P+*, B2. The effect of solvent was systematically estimated using the SCRF model, based on the Poisson−Boltzmann equation, as implemented in JAGUAR5.5.[25] This model defines the solvent by two parameters, a dielectric constant (ϵ) and a probe radius (r); the program calculates the cavity of the solute. We used to solvents a, $\epsilon = 5.7$, $r = 2.7$ Å, and b, $\epsilon = 37.5$ (as for acetonitrile), $r = 2.2$ Å.

Acknowledgment. This research was supported by the German Federal Ministry of Education and Research (BMBF) within the framework of the German-Israeli Project Cooperation (DIP-G7.1) and the Helen and Martin Kimmel Center for Molecular Design. R.N. is the Rebbeca and Israel Sieff Professor of Organic Chemistry.

Supporting Information Available: Figures (21) and tables (36) of the structure, energy profiles, charges, and spin densities calculated for this study. This material is available free of charge via the Internet at http://pubs.acs.org.

JA0638455